
Dynamic Stability Analysis of a Circularly Tapered Rotating Beam Subjected to Axial Pulsating Load and Thermal Gradient under Various Boundary Conditions

Rashmita Parida

Department of Mechanical Engineering, College of Engineering and Technology, Bhubaneswar Techno Campus, Ghatikia, Bhubaneswar, Orissa, India-751003

Pusparaj Dash

Department of Mechanical Engineering, VSSUT Burla, Sambalpur, Orissa, India-768018

(Received 13 August 2013; accepted 8 October 2015)

The dynamic stability of a circularly tapered rotating beam subjected to a pulsating axial external excitation with thermal gradient was studied for all possible combinations of clamped, guided, pinned, fixed, and free boundary conditions. The equations of motion and associated boundary conditions were obtained using the extended Hamilton's principle. Then these equations of motion and the associated boundary conditions were non-dimensionalised. A set of Hill's equations were obtained from the non-dimensional equations of motion by the application of the extended Galerkin method. The zones of parametric instability were obtained using Saito-Otomi conditions. The effects of various boundary conditions, thermal gradient, taper, and rotational speed on the regions of parametric instability were investigated and presented through a series of graphs. The results reveal that increasing rotational speed and taper have stabilizing effects, whereas increasing thermal gradient has a destabilizing effect for all boundary conditions of the beam.

NOMENCLATURE

$A(x), A(\xi)$	Area of a generic section of the beam
A_1	Cross sectional area at the end $x = l$
C_0	Hub radius
c_0	Dimensionless hub radius, $= C_0/l$
$d(x), d(\xi)$	Diameter of a generic section of the beam
d_1	Diameter at the end, $x = l$
$E(x), E(\xi)$	Young's modulus at a generic section
E_1	Young's modulus at the end, $x = l$
$I(x), I(\xi)$	Moment of inertia at a generic section
I_1	Moment of inertia at the end, $x = l$
l	Length of the beam
$m(\xi)$	Mass distribution function
P_0	Static axial load
P_1	Dynamic axial load
$p(\tau)$	Dimensionless load
p_0	Dimensionless static axial load
p_1	Dimensionless dynamic axial load
$S(\xi)$	Moment of inertia distribution function
$T(\xi)$	Elasticity modulus distribution function
t	Time
$w(x, t)$	Transverse deflection of the beam
γ	Coefficient of thermal expansion of the beam material
δ	Thermal gradient parameter
a^*	Diameter taper parameter
η	Dimensionless transverse deflection, $= w/l$
ξ	Dimensionless length, $= x/l$
τ	Dimensionless time, $= ct$
ρ	Density of the beam material

Ω	Uniform angular velocity Ω of the beam about z' -axis
Ω_0	Rotational speed parameter
ω	Excitation frequency
ω_0	Dimensionless fundamental natural frequency
Θ	Non-Dimensional excitation frequency, $= \omega/c$
Ψ_0	Reference temperature
Ψ_1	Temperature at the end, $\xi = 1$

1. INTRODUCTION

The stability analysis and dynamic behaviour of a rotating cantilever beam with axial orientation perpendicular to the axis of spin is very essential for its practical applications such as turbomachinery blades, rotor blades of helicopter, aircraft propellers, flexible appendages of spacecraft, satellite antennas, and robotic manipulators, to name a few. In some cases the structures have to operate under elevated temperatures. A linear relation is observed between the Young's modulus and the temperature of most engineering materials.

An ample number of publications are available regarding the design and analysis of rotating structures. The flexural vibrations of a rotating cantilever beam with a tip mass at the free end has been studied by Bhat.¹ He proposed the beam characteristic orthogonal polynomials in the Rayleigh-Ritz method. Liu and Yeh² have investigated the influence of restrained parameters on the Eigen frequencies of rotating uniform and non-uniform beams with a restrained base using Galerkin's method. The stability analysis of a rotating shaft due to pulsating torque applied at its end has been studied by Unger and

Brull.³ They found that instability arising from the combination resonance has the most adverse effect. Kammer and Schlack⁴ adopted the Krylov-Bogoliubov-Mitropolskii (KBM) perturbation technique to solve the problem of instability due to the time dependent angular velocity in a rotating Euler beam. Namachchivaya⁵ investigated the dynamic stability of rotating shaft under the excitation of combined harmonic and stochastic load and derived the stability conditions explicitly for the first and second order moments considering the shaft as a two degrees of freedom system. Bauer and Eidel⁶ studied the effects on vibration and buckling of a rotating Euler beam of uniform cross section because of its spin speed, hub radius and aspect ratio considering an orientation perpendicular to the axis of rotation. The dynamic stability analysis of rotating Timoshenko beam with a root flexibility using finite element method was investigated for the first time by Abbas.⁷ Ishida *et al.*⁸ studied the vibration and stability of a rotating shaft under a sinusoidal axial force assuming a four degrees of freedom system. The stability of a tapered cantilever beam on Winkler foundation subjected to a follower force was studied by Lee.⁹ He found that the critical flutter loads of both tapered beams and beams of a uniform cross section are unaffected by the presence of viscous damping in the elastic foundation. Lin and Chen¹⁰ studied the dynamic stability of rotating composite beams using finite element method. Tan *et al.*¹² discussed the instability of a spinning pre-twisted beam under compressive axial loads assuming Euler-Bernoulli beam theory (EBT) and assumed mode method. Banerjee *et al.*¹² applied the dynamic stiffness method to analyse the free vibration of a rotating taper beam that follows EBT. They derived some explicit analytical expressions and used the Wittrick-Williams algorithm for the solution. Shahba and Rajasekaran¹³ used the differential transform element method (DTEM) and differential quadrature element method (DQEL) of lower order to solve the equations of free vibration and stability of tapered Euler-Bernoulli beam made of axially functionally graded material. Yang *et al.*¹⁴ developed a finite element model to study the free vibration of a rotating uniform Euler-Bernoulli beam. They considered the coupling of axial and transverse vibration and of elastic deformations and rigid motion. Nayak *et al.*¹⁵ investigated the stability of a sandwich beam on viscoelastic supports subjected to a pulsating axial load with temperature gradient. Soltani *et al.*¹⁶ proposed a numerical solution based on power series method to derive the critical buckling loads and frequency of free vibrations for tapered thin beams. Bulut¹⁷ studied the dynamic stability of parametrically excited rotating tapered beam and found that the number of instability zones increases with the taper ratio.

A survey of literature reveals that some work has been done on parametric instability and dynamic stability of a symmetric rotating beam, parametric instability of a non-uniform beam with thermal gradient resting on a Pasternak foundation, and that of a symmetric sandwich beam for different boundary conditions. However, no work has been done to study the static and dynamic stability of a rotating tapered beam with thermal gradient under various boundary conditions. Thus the present work mainly deals with a theoretical study of a rotating tapered beam with a pulsating load and thermal gradient under various boundary conditions. The static and dynamic stability of a rotating tapered cantilever beam which is fixed at one end and subjected to an axial pulsating load and a steady, one-

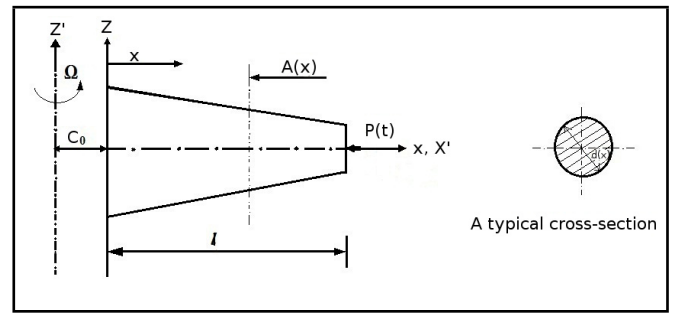


Figure 1. System Configuration.

dimensional temperature gradient at the free end has been reported. The effect of the rotation parameter, geometric parameters, taper parameter, and the thermal gradient on the non-dimensional static buckling loads zones and also on the parametric instability zones are investigated.

2. FORMULATION OF THE PROBLEM

2.1. System Configuration

A rotating tapered cantilever beam of length l set off a distance C_0 from the axis of rotation which rotates at a uniform angular velocity Ω about a vertical z' -axis is capable of oscillating in the $x-z$ plane. The beam is oriented along the x -axis perpendicular to the axis of rotation as shown in Fig. 1. A pulsating axial force $P(t) = P_0 + P_1 \cos \omega t$ is applied at the end $x = C_0 + l$ of the beam along the point of C.G. of the cross-section in the axial direction, with ω being the frequency of the applied load, t being the time, and P_0 and P_1 being the static and dynamic load amplitudes, respectively.

The following assumptions are made for deriving the equations of motion:

- The material of the beam is homogeneous & isotropic in nature.
- The deflections of the beam are small and the transverse deflection $w(x, t)$ is the same for all points of a cross-section.
- The beam obeys Euler-Bernoulli beam theory.
- Extensional deflection of the beam is neglected.
- A steady one-dimensional temperature gradient is assumed to exist along the central length of the beam.
- Extension and rotary inertia effects are negligible.

The expressions for potential energy, kinetic energy and work done are as follows:

$$V = \frac{1}{2} \int_0^l E(x)I(x) \left(\frac{\partial^2 w}{\partial x^2} \right)^2 dx + \frac{1}{2} \int_0^l \rho A(x) \Omega^2 (C_0 + x) \int_0^{x'} \left(\frac{\partial w}{\partial x} \right)^2 dx; \quad (1)$$

$$T = \frac{1}{2} \int_0^l \rho A(x) \left(\frac{\partial w}{\partial t} \right)^2 dx + \frac{1}{2} \int_0^l \rho \Omega^2 A(x) w^2 dx; \quad (2)$$

$$W_P = \frac{1}{2} \int_0^l P(t) \left(\frac{\partial w}{\partial x} \right)^2 dx; \tag{3}$$

where $w(x, t)$ is transverse deflection of the beam.

The application of the extended Hamilton's principle gives the following equation of motion and boundary conditions:

$$\delta \int_{t_1}^{t_2} (T - V - W_P) dt = 0; \tag{4}$$

$$[E(x) I(x) w_{,xx}]_{,xx} + \rho A(x) w_{,tt} + \rho \Omega^2 I(x) w_{,xx} - [N(x_1) w_{,x}]_{,x} + P(t) w_{,xx} = 0; \tag{5}$$

where $N(x_1) = \frac{1}{2} \rho A(x) \Omega^2 [(C_0 + l)^2 - (C_0 + x')^2]$. The boundary conditions at $x = C_0$ and $x = C_0 + l$ are

$$\begin{aligned} [E(x) I(x) w_{,xx}]_{,x} + P(t) w_{,x} &= 0; \\ [E(x) I(x) w_{,xx}]_{x=l} &= 0; \\ w_{,t} &= 0. \end{aligned} \tag{6}$$

In the above expression $w_{,x} = \frac{\partial w}{\partial x}$, $w_{,xx} = \frac{\partial^2 w}{\partial x^2}$, $w_{,t} = \frac{\partial w}{\partial t}$, $w_{,tt} = \frac{\partial^2 w}{\partial t^2}$.

Introducing the dimensionless parameters,

$$\xi = \frac{x}{l}, \eta = \frac{w}{l}, c_0 = \frac{C_0}{l}, \tau = ct;$$

$$\left(\because c^2 = \frac{E(x) I(x)}{\rho A(x) l^4} \right);$$

$$\frac{\partial w}{\partial x} = \frac{\partial \eta}{\partial \xi} \text{ and } \left(\frac{\partial w}{\partial x} \right)^2 = \left(\frac{\partial \eta}{\partial \xi} \right)^2;$$

$$\frac{\partial^2 w}{\partial x^2} = \frac{1}{l} \frac{\partial^2 \eta}{\partial \xi^2} \text{ and } \left(\frac{\partial^2 w}{\partial x^2} \right)^2 = \frac{1}{l^2} \left(\frac{\partial^2 \eta}{\partial \xi^2} \right)^2;$$

$$\frac{\partial w}{\partial t} = cl \left(\frac{\partial \eta}{\partial \tau} \right) \text{ and } \left(\frac{\partial w}{\partial t} \right)^2 = c^2 l^2 \left(\frac{\partial \eta}{\partial \tau} \right)^2;$$

$$p(\tau) = \frac{P(t) l^2}{E_1 I_1}, p(\tau) = p_0 + p_1 \cos \theta \tau;$$

$$(\cdot)' = \frac{\partial(\cdot)}{\partial \xi}, (\cdot) \dot{} = \frac{\partial(\cdot)}{\partial \tau}, \text{ etc.}$$

The non dimensional equation of motion and boundary conditions can be written as

$$[S(\xi) T(\xi) \eta''']'' + m(\xi) \ddot{\eta} + [r_g \Omega_0^2 + p(\tau)] \eta'' - \Omega_0^2 [q(\xi) \eta']' = 0; \tag{7}$$

and

$$\begin{aligned} \{[S(\xi) T(\xi) \eta''']' + p(\tau) \eta'\}_{\xi=1} &= 0; \\ [S(\xi) T(\xi) \eta''']_{\xi=1} &= 0; \\ \eta(0, \tau) &= 0; \\ \eta'(0, \tau) &= 0. \end{aligned} \tag{8}$$

In the above expressions $r_g = \frac{I(\xi)}{A_1 l^2}$; $\Omega_0^2 = \frac{\rho A(\xi) \Omega^2 l^4}{E_1 I_1}$;

$$\Omega_0^2 q(\xi) = \frac{N(x_1) l^2}{E_1 I_1}; A(\xi) = A_1 m(\xi), E(\xi) = E_1 T(\xi), I(\xi) = I_1 S(\xi).$$

2.2. Approximate Solution

The approximate solution to the non dimensional equations of motion is assumed as

$$\eta(\xi, \tau) = \sum_{r=1}^N \eta_r(\xi) f_r(\tau); \tag{9}$$

where $f_r(\tau)$ is an unknown function of time and $\eta_r(\xi)$ is a coordinate function to be chosen so as to satisfy as many of the boundary conditions in Eq. (8) as possible. It is further assumed that $\eta_r(\xi)$ can be represented by a set of functions (9) which satisfy the conditions obtained from Eq. (7) by deleting the terms containing ω_0 and $p(\tau)$. It is further assumed that coordinate functions for the various boundary conditions can be approximated by the ones given in Table 1.

Substitution of the series of solutions in the non dimensional equations of motion and subsequent application of the general Galerkin method leads to the following matrix equations of motion:

$$[M] \{\ddot{f}\} + [K] \{f\} - \{p_0 [H] - p_1 \cos \theta \tau [H]\} \{f\} = \{0\}; \tag{10}$$

where $\ddot{f} = \frac{\partial^2 f}{\partial \tau^2}$ and $\{f\} = \{f_1, \dots, f_N\}^T$. The various matrix elements are given by $\int_0^1 m(\xi) \eta_i(\xi) \eta_j(\xi) d\xi = M_{ij}$;

$$\int_0^1 \left\{ S(\xi) T(\xi) \eta_i''(\xi) \eta_j''(\xi) + \Omega_0^2 [q(\xi) - r_g] \eta_i'(\xi) \eta_j'(\xi) \right\} d\xi = K_{ij};$$

$$\int_0^1 \eta_i'(\xi) \eta_j'(\xi) d\xi = H_{ij}; \text{ and}$$

$$\because i, j = 1, 2, \dots, N.$$

2.3. Regions of Dynamic Instability

Let $[L]$ be the modal matrix of $[M]^{-1}[K]$. Then by the introduction of the linear coordinate transformation, $\{f\} = [L]\{v\}$, $\{v\}$ being a new set of generalized coordinates yields,

$$\{\ddot{v}\} + [\omega_n^2] \{v\} + p_1 \cos(\theta \tau) [B] \{v\} = \{0\}; \tag{11}$$

where $[\omega_n^2]$ is a spectral matrix corresponding to $[m]^{-1}[k]$ and $[B] = -[L]^{-1}[M]^{-1}[H][L]$.

Equation (11) can be written as,

$$\ddot{v}_n + \omega_n^2 v_n + p_1 \cos(\theta \tau) \sum_{m=1}^{m=N} b_{nm} u_n = 0, \quad n = 1, 2, \dots, N \tag{12}$$

Equation (12) represents a system of N coupled Hill's equations with complex coefficients.

Here, ω_n and b_{nm} are complex quantities, given by $\omega_n = \omega_{n,R} + j\omega_{n,I}$; $b_{n,m} = b_{nm,R} + jb_{nm,I}$.

The boundaries of the region of instability of simple and combination resonances are obtained using the following conditions by Saito & Otomi.¹⁸

Case (A): Simple resonance

In this case, the regions of instability are given: When damping is present.

$$\left| \frac{\theta}{2} - \omega_{\mu,R} \right| < \frac{1}{4} \sqrt{\frac{\overline{P}_1^2 (b_{\mu\mu,R}^2 + b_{\mu\mu,I}^2)}{\omega_{\mu,R}^2} - 16\omega_{\mu,I}^2}. \tag{13}$$

And, for the undamped case,

$$\left| \frac{\theta}{2} - \omega_{\mu,R} \right| < \frac{1}{4} \frac{|\overline{P}_1 b_{\mu\mu,R}|}{\omega_{\mu,R}}. \tag{14}$$

Table 1. Coordinate functions.

End arrangement	Coordinate function $i = 1, 2, \dots, r$
P-P	$\eta(\xi) = \sin(\pi i \xi)$
G-P	$\eta(\xi) = \cos\{(2i - 1)\pi \xi / 2\}$
C-P	$\eta(\xi) = 2(i + 2)\xi^{(i+1)} - (4i + 6)\xi^{(i+2)} + 2(i + 1)\xi^{(i+3)}$
C-C	$\eta(\xi) = \xi^{(i+1)} + 2\xi^{(i+2)} + \xi^{(i+3)}$
C-CUR	$\eta(\xi) = (i + 3)(i + 2)^2(i + 1)\{\xi^{(i+1)} - 2\xi^{(i+2)} + \xi^{(i+3)}\}$
C-F	$\eta(\xi) = (i + 2)(i + 3)\xi^{(i+1)} - 2i(i + 3)\xi^{(i+2)} + i(i + 1)\xi^{(i+2)}$

for $\mu = 1, 2, \dots, N$.

Case (B): Combination resonance of the sum type

This type of resonance occurs when $\mu \neq v$; $\mu, v = 1, 2, \dots, N$ and the regions of instability are given:

For the damped case,

$$\left| \frac{\omega}{2} - \frac{1}{2}(\omega_{\mu,R} + \omega_{v,R}) \right| < \frac{\omega_{\mu,I} + \omega_{v,I}}{8\sqrt{\omega_{\mu,I}\omega_{v,I}}} \sqrt{\frac{\bar{P}_1^2}{\omega_{\mu,R}\omega_{v,R}} (b_{\mu v,R}b_{v\mu,R} + b_{\mu v,I}b_{v\mu,I}) - 16\omega_{\mu,I}\omega_{v,I}} \quad (15)$$

For the undamped case,

$$\left| \frac{\omega}{2} - \frac{1}{2}(\omega_{\mu,R} + \omega_{v,R}) \right| < \frac{\bar{P}_1}{4} \sqrt{\frac{b_{\mu v,R}b_{v\mu,R}}{\omega_{\mu,R}\omega_{v,R}}} \quad (16)$$

Case(C): Combination resonance of the difference type

This type of resonance occurs when $\mu < v$, ($\mu, v = 1, 2, \dots, N$) and the regions of instability are given:

For the damped case,

$$\left| \frac{\omega}{2} - \frac{1}{2}(\omega_{v,R} - \omega_{\mu,R}) \right| < \frac{\omega_{\mu,I} + \omega_{v,I}}{8\sqrt{\omega_{\mu,I}\omega_{v,I}}} \sqrt{\frac{\bar{P}_1^2}{\omega_{\mu,R}\omega_{v,R}} (-b_{\mu v,R}b_{v\mu,R} + b_{\mu v,I}b_{v\mu,I}) - 16\omega_{\mu,I}\omega_{v,I}} \quad (17)$$

For the undamped case,

$$\left| \frac{\omega}{2} - \frac{1}{2}(\omega_{v,R} - \omega_{\mu,R}) \right| < \frac{\bar{P}_1}{4} \sqrt{\frac{-b_{\mu v,R}b_{v\mu,R}}{\omega_{\mu,R}\omega_{v,R}}} \quad (18)$$

Dynamic stability analysis of the circularly tapered rotating beam with axial pulsating load and thermal gradient under various boundary conditions has been carried out by using Eqs. (14), (16), and (18). From them, regions of instability are obtained for various cases.

3. NUMERICAL RESULTS AND DISCUSSIONS

Numerical results were obtained for various values of the parameters like rotation parameter, geometric parameter, taper parameter, and thermal gradient. The linearly tapered cantilever beam with a circular cross-section is assumed to have a diameter varying according to the relation $d(\xi) = d_1[1 + \alpha^*(1 - \xi)]$, where d_1 is the diameter of the beam at the end $\xi = 1$, and α^* is the diameter taper parameter.

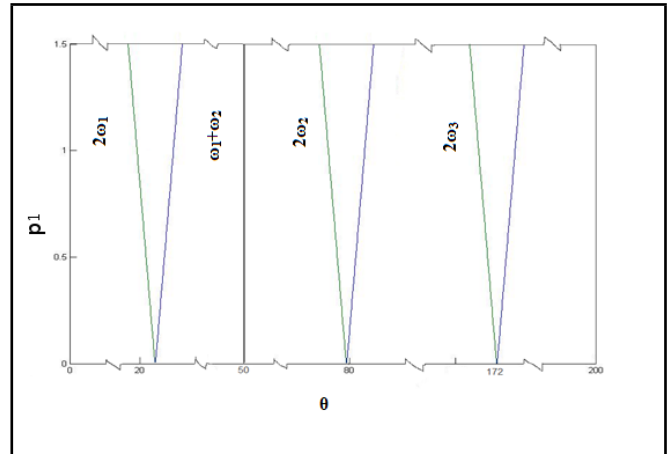


Figure 2. Stability diagram for pinned-pinned beam with $\Omega_0 = 5$ ($\delta = 0.1$, $\alpha^* = 2$).

Consequently, the mass distribution $m(\xi)$ and the moment of inertia distribution $S(\xi)$ are given by the relations

$$m(\xi) = [1 + \alpha^*(1 - \xi)]^2; \quad S(\xi) = [1 + \alpha^*(1 - \xi)]^4.$$

The temperature above the reference temperature at any point ξ from the end of the beam is assumed to be $\Psi = \Psi_0(1 - \xi)$. Choosing $\Psi_0 = \Psi_1$, the temperature at the end $\xi = 1$, as the reference temperature, means the variation of modulus of elasticity of the beam is denoted by

$$E(\xi) = E_1 [1 - \gamma\Psi_1 (1 - \xi)], \quad 0 \leq \gamma\Psi_1 < 1; \quad E(\xi) = E_1 T(\xi),$$

where γ is the coefficient of thermal expansion of the beam material, $\delta = \gamma\Psi_1$ is the thermal gradient parameter, and $T(\xi) = [1 - \delta(1 - \xi)]$, where δ is the thermal gradient along the length of the beam.

The dynamic stability analysis of the system for various boundary conditions has been analysed as follows:

If, for the change in value of a parameter, the width of the instability zone increases or the zone is pulled down or shifted towards a lower excitation frequency region, the stability of the system worsens. Otherwise, if with the change in the value of the parameter, the width of the instability zone decreases or is pulled up or shifted towards the higher excitation frequency region, or if the number of instability zones reduces, then the stability of the system improves. With these above conditions, the effect of various parameter on the dynamic stability of the system have been analysed.

The regions of parametric instability of a beam with various boundary conditions for two different values of rotational speed parameters are shown in Figs. 2, 3, 5, 6, 8, 9, 11, 12, 14, 15, 17, and 18.

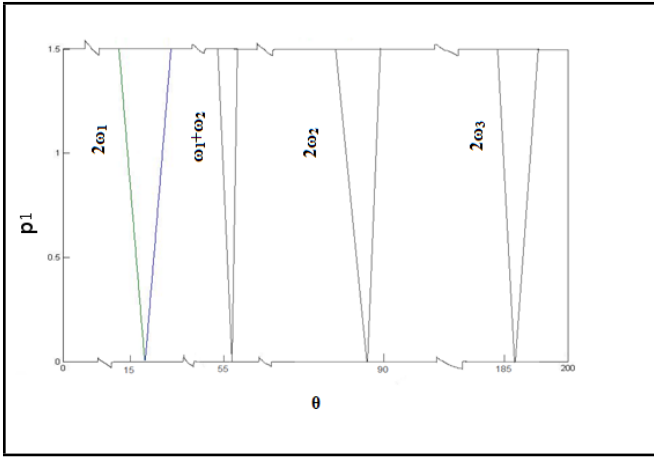


Figure 3. Stability diagram for pinned-pinned beam with $\Omega_0 = 15$ ($\delta = 0.1$, $\alpha^* = 2$).

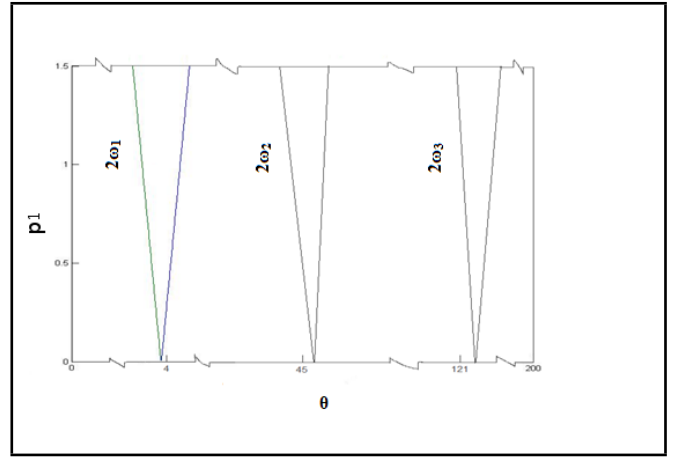


Figure 6. Stability diagram for guided-pinned beam with $\Omega_0 = 5$ ($\delta = 0.1$, $\alpha^* = 2$).

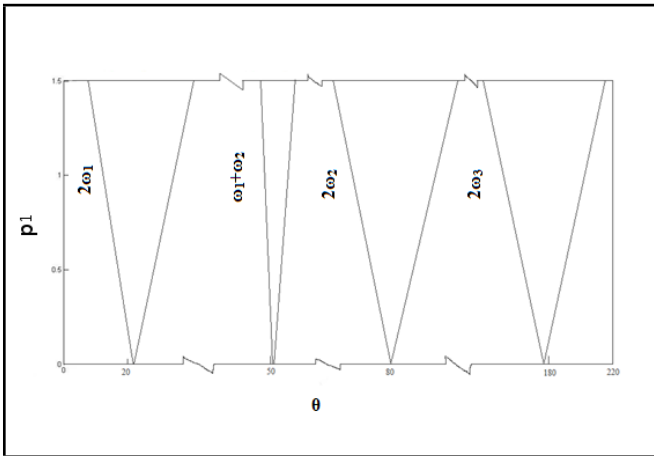


Figure 4. Stability diagram for pinned-pinned beam with $\Omega_0 = 5$ ($\delta = 0.4$, $\delta = 0.8$, $\alpha^* = 1$).

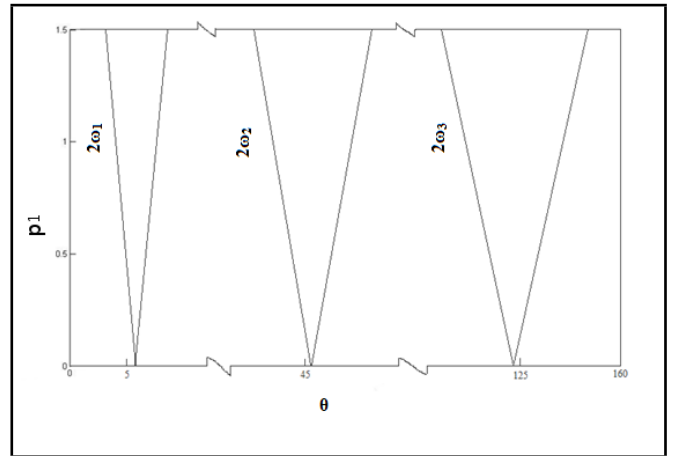


Figure 7. Stability diagram for guided-pinned beam with $\Omega_0 = 5$ ($\delta = 0.4$, $\delta = 0.8$, $\alpha^* = 1$).

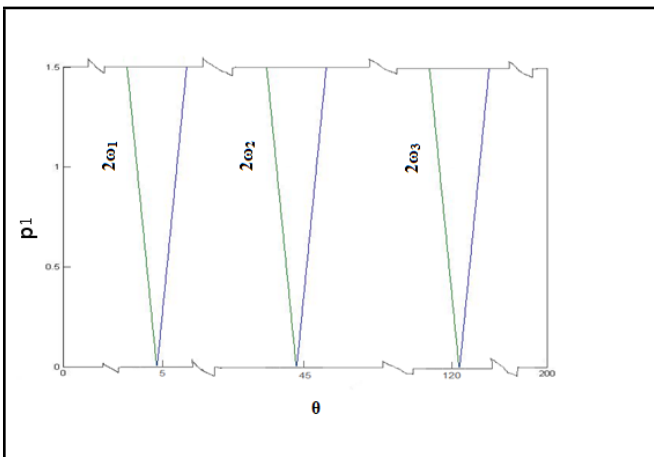


Figure 5. Stability diagram for guided-pinned beam with $\Omega_0 = 2$ ($\delta = 0.1$, $\alpha^* = 2$).

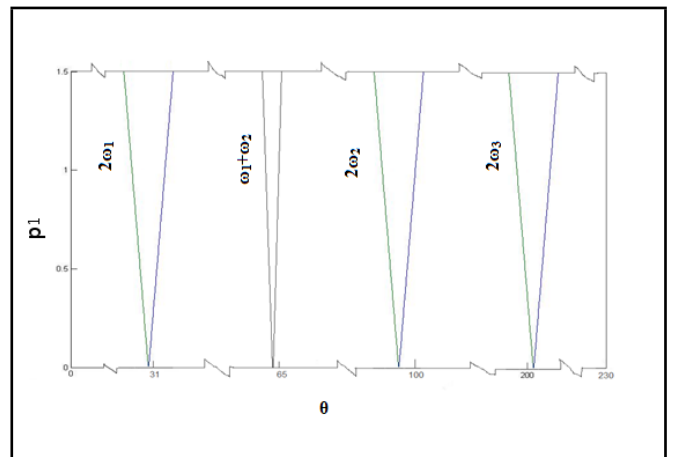


Figure 8. Stability diagram for clamped-pinned beam with $\Omega_0 = 5$ ($\delta = 0.1$, $\alpha^* = 2$).

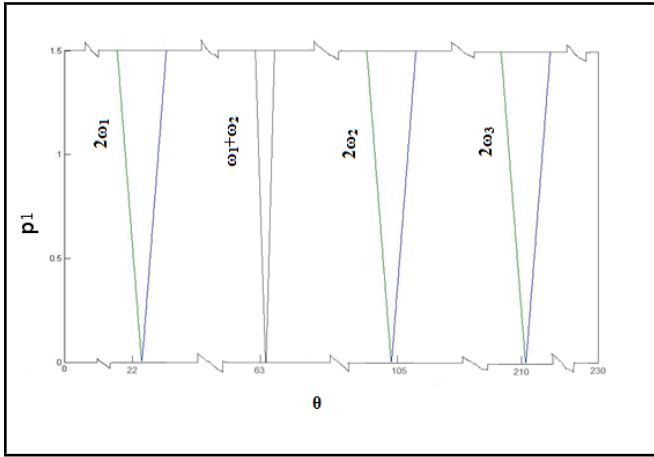


Figure 9. Stability diagram for clamped-pinned beam with $\Omega_0 = 15$ ($\delta = 0.1$, $\alpha^* = 2$).

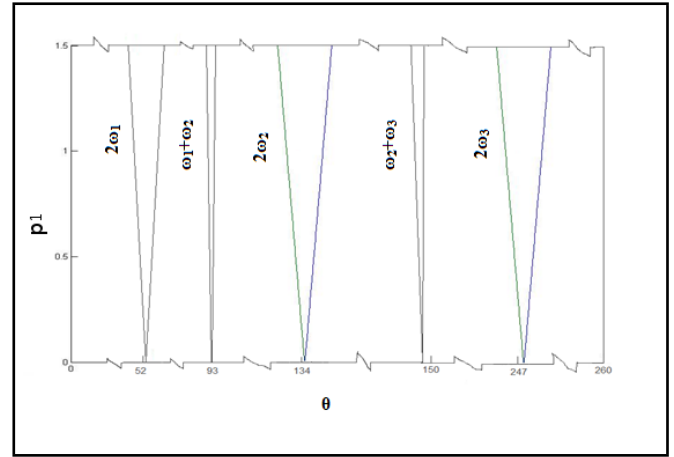


Figure 12. Stability diagram for clamped-clamped beam with $\Omega_0 = 15$ ($\delta = 0.1$, $\alpha^* = 2$).

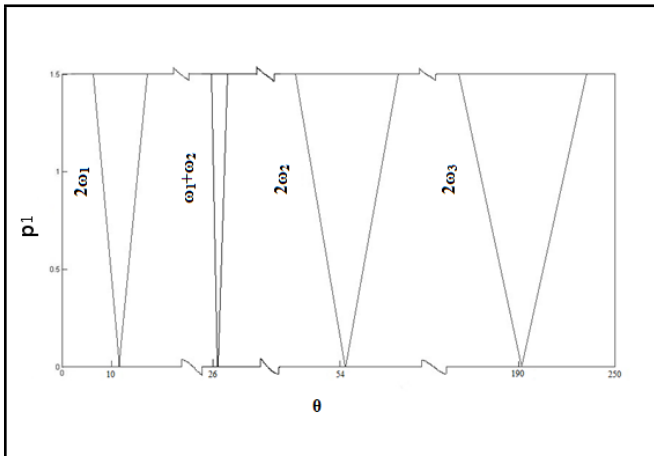


Figure 10. Stability diagram for clamped-pinned beam with $\Omega_0 = 5$ ($\delta = 0.4$, $\delta = 0.8$, $\alpha^* = 1$).

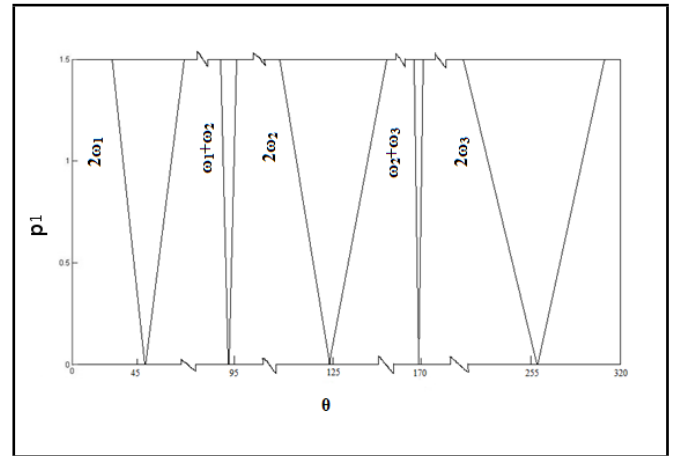


Figure 13. Stability diagram for clamped-clamped beam with $\Omega_0 = 5$ ($\delta = 0.4$, $\delta = 0.8$, $\alpha^* = 1$).

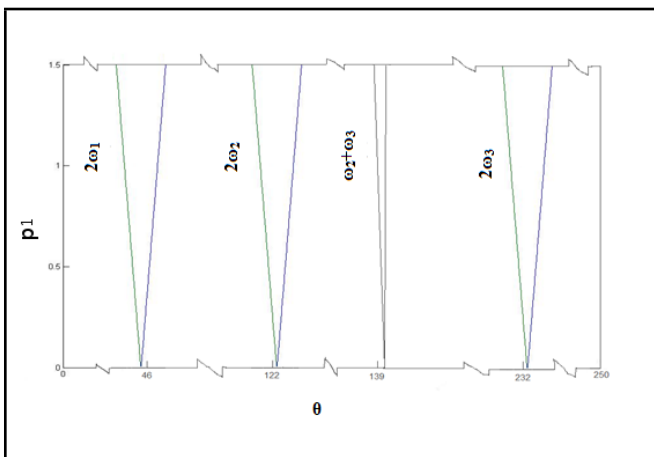


Figure 11. Stability diagram for clamped-clamped beam with $\Omega_0 = 5$ ($\delta = 0.1$, $\alpha^* = 2$).

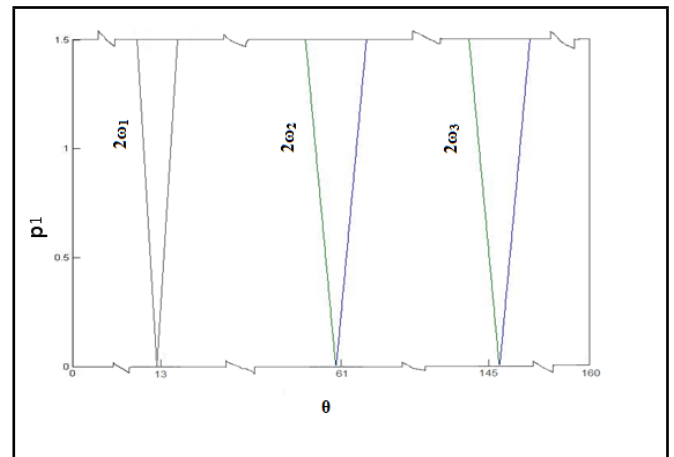


Figure 14. Stability diagram for clamped-CUR beam with $\Omega_0 = 5$ ($\delta = 0.1$, $\alpha^* = 2$).

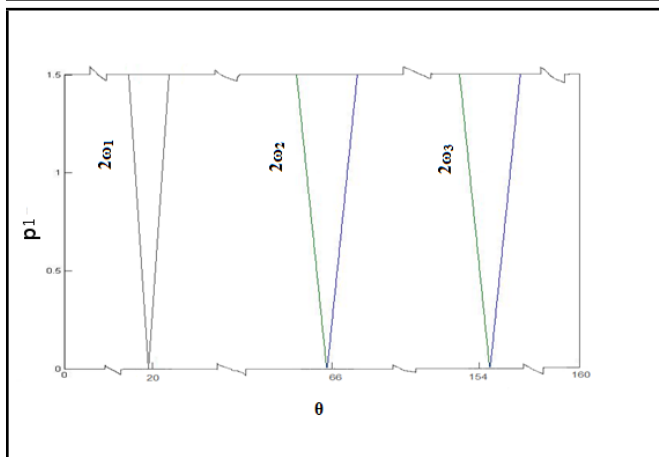


Figure 15. Stability diagram for clamped-CUR beam with $\Omega_0 = 15$ ($\delta = 0.1$, $\alpha^* = 2$).

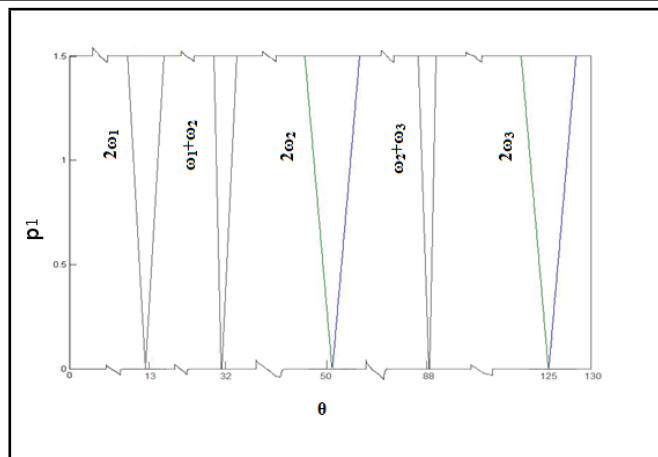


Figure 17. Stability diagram for clamped-free beam with $\Omega_0 = 5$ ($\delta = 0.1$, $\alpha^* = 2$).

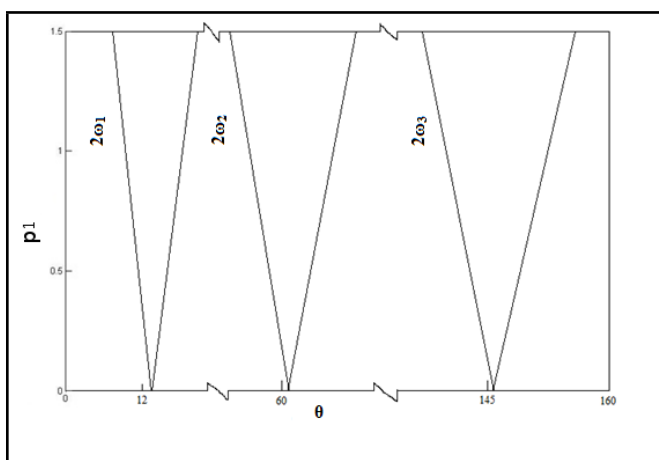


Figure 16. Stability diagram for clamped-CUR beam with $\Omega_0 = 5$ ($\delta = 0.4$, $\delta = 0.8$, $\alpha^* = 1$).

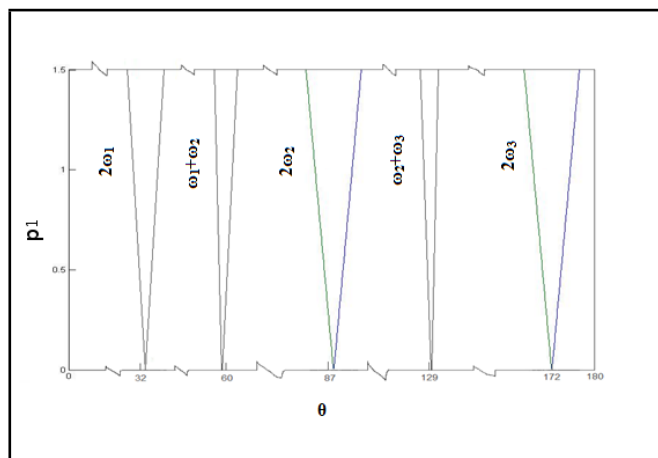


Figure 18. Stability diagram for clamped-free beam with $\Omega_0 = 15$ ($\delta = 0.1$, $\alpha^* = 2$).

Combination resonances of the difference-type do not occur in any of the cases under consideration. While an increase in the value of Ω_0 reduces the width of the first-order simple resonance zones of clamped-clamped beam, it widens some of the combination resonance zones and shifts all the regions to higher excitation frequencies. The combination resonance regions at $\Theta = (\omega_3 + \omega_1)$ of a clamped-clamped beam reduce in width due to the increase in angular velocity. For a beam with clamped-free end conditions, a higher rotational speed reduces the span of most of the instability regions and makes the beam less susceptible to periodic forces by relocating them at higher frequencies, whereas a rise in the rotational speed increases the span of most of the instability regions of a clamped-pinned beam and relocates them at higher excitation frequencies. On the other hand, it repositions those around $2\omega_1$ and $(\omega_1 + \omega_2)$ at lower frequencies and reduces the width of the ones at $\Theta = 2\omega_2$, $2\omega_3$ and $(\omega_3 + \omega_1)$. With increase in the angular velocity of pinned-pinned beam, most of the resonance zones are widened, but those near $\Theta = 2\omega_2$ and $2\omega_3$ are reduced in span. Further, while the instability regions in the vicinities of $2\omega_1$ shifts to lower frequencies, all others are repositioned at higher ones.

From the figures, it is observed that increase in rotational speed parameter stabilizes the beams with pinned-pinned, clamped-clamped, clamped-clamped unrestrained, and

clamped-free conditions, whereas it has a destabilizing effect on guided-pinned and clamped-pinned beams.

The influence of taper parameter and thermal gradient parameter on the principal region of instability is shown in Figs. 4, 7, 10, 13, 16, and 19. The figures show the effect of two values of the thermal gradient parameter δ on the instability regions for taper parameter $\alpha^* = 1$ for all the considered boundary conditions. It has been observed that, for all cases, the instability regions experience a slight increase in width and shift towards lower excitation frequencies with an increase in the value of δ .

4. CONCLUSION

A computational analysis of the dynamic stability of a tapered cantilever beam with pulsating axial load and thermal gradient under various boundary conditions was considered. The programming was developed using MATLAB. The following are the conclusions drawn from the study.

The dynamic stability of a rotating tapered beam under a pulsating axial load was investigated for all possible combinations of clamped, guided, pinned, and free boundary conditions. Results reveal that, a higher rotational speed make a clamped-free beam less sensitive to periodic forces. While rise in the angular velocity reduces the intensity of the simple resonances of clamped-clamped beam, it increases the severity of

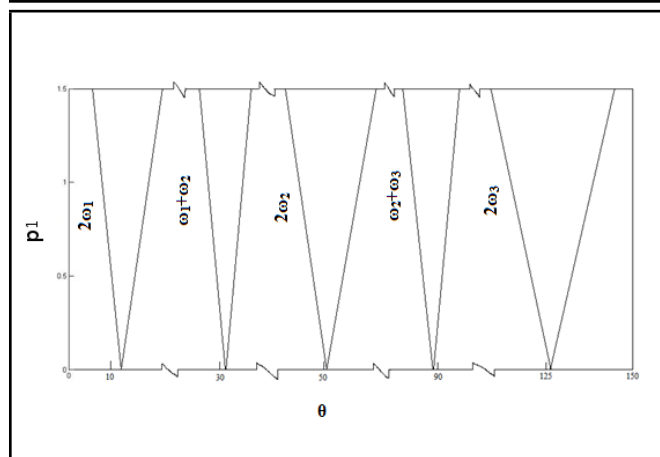


Figure 19. Stability diagram for clamped-free beam with $\Omega_0 = 5$ ($\delta = 0.4$, $\delta = 0.8$, $\alpha^* = 1$).

some of the combination resonances. It is also observed that clamped-pinned and pinned-pinned beams may either stabilize or destabilize with an increase in rotational speed.

An increase in taper parameter reduces the widths of the principal regions of instability and shifts them towards higher excitation frequencies, thus making the beam less sensitive to periodic forces. However, an increase in thermal gradient widens the principal regions of instability, shifting them towards lower excitation frequencies, thereby making the beam more sensitive to periodic forces. Thus, it may be inferred that increasing taper has stabilizing effects on the beams, whereas increasing temperature gradient has a destabilizing effect on the beams of all cases.

REFERENCES

- 1 Bhat, R. B. Transverse vibrations of a rotating uniform cantilever beam with tip mass as predicted by using beam characteristic orthogonal polynomials in the Rayleigh-Ritz method, *J. Sound Vib.*, **105**, 199–210, (1986). [http://dx.doi.org/10.1016/0022-460x\(86\)90149-5](http://dx.doi.org/10.1016/0022-460x(86)90149-5)
- 2 Liu, W. H. and Yeh, F.-H. Vibrations of non-uniform rotating beams, *J. Sound Vib.*, **119**, 379–384, (1987). [http://dx.doi.org/10.1016/0022-460x\(87\)90463-9](http://dx.doi.org/10.1016/0022-460x(87)90463-9)
- 3 Unger, A. and Brull, M. A. Parametric instability of a rotating shaft due to pulsating torque, *J. Appl. Mech., Trans. ASME*, **48**, 948–958, (1981). <http://dx.doi.org/10.1115/1.3157761>
- 4 Kammer, D. C. and Schlack, Jr., A. L. Dynamic Response of a Radial Beam With Nonconstant Angular Velocity, *J. Vib. Acoust., Stress, Reliab. Des., Trans. ASME*, **109**, 138–143, (1987). <http://dx.doi.org/10.1115/1.3269405>
- 5 Namachchivaya, N. S. Mean square stability of a rotating shaft under combined harmonic and stochastic excitations, *J. Sound Vib.*, **133**, 323–336 (1989). [http://dx.doi.org/10.1016/0022-460x\(89\)90929-2](http://dx.doi.org/10.1016/0022-460x(89)90929-2)
- 6 Bauer, H. F. and Eidel, W. Vibration of a rotating uniform beam, Part II: Orientation perpendicular to the axis of rotation, *J. Sound Vib.*, **122**, 357–375 (1988). [http://dx.doi.org/10.1016/s0022-460x\(88\)80360-2](http://dx.doi.org/10.1016/s0022-460x(88)80360-2)
- 7 Abbas, B. A. H. Dynamic stability of a rotating Timoshenko beam with a flexible root, *J. Sound Vib.*, **108**, 25–32 (1986). [http://dx.doi.org/10.1016/s0022-460x\(86\)80308-x](http://dx.doi.org/10.1016/s0022-460x(86)80308-x)
- 8 Ishida, Y., Ikeda, T., Yamamoto, T., and Esaka, T. Parametrically Excited Oscillations of a Rotating Shaft Under a Periodic Axial Force, *JSME Int. J.*, **31** (4), 698–704 (1988). <http://dx.doi.org/10.1299/jsmec1988.31.698>
- 9 Lee, H. P. Dynamic stability of a tapered cantilever beam on an elastic foundation subjected to a follower force, *Int. J. Solids Structures*, **33** (10), 1409–1424, (1996). [http://dx.doi.org/10.1016/0020-7683\(95\)00108-5](http://dx.doi.org/10.1016/0020-7683(95)00108-5)
- 10 Lin, C. Y. and Chen, L. W. Dynamic stability of rotating composite beams with a viscoelastic core, *Compos. Struct.*, **58** (2), 185–194, (2002). [http://dx.doi.org/10.1016/s0263-8223\(02\)00127-7](http://dx.doi.org/10.1016/s0263-8223(02)00127-7)
- 11 Tan, T. H., Lee, H. P. and Leng, G. S. B. Parametric instability of spinning pretwisted beams subjected to sinusoidal compressive axial loads, *Compos. Struct.*, **66** (6), 745–764, (1998). [http://dx.doi.org/10.1016/s0045-7949\(98\)00002-9](http://dx.doi.org/10.1016/s0045-7949(98)00002-9)
- 12 Banerjee, J. R., Su, H., and Jackson, D. R. Free vibration of rotating tapered beams using the dynamic stiffness method, *J. Sound Vib.*, **298** (4–5) 1034–1054, (2006). <http://dx.doi.org/10.1016/j.jsv.2006.06.040>
- 13 Shahba, A. and Rajasekaran, S. Free vibration and stability of tapered Euler–Bernoulli beams made of axially functionally graded materials, *Appl. Math. Model.*, **36** (7), 3094–3111, (2012). <http://dx.doi.org/10.1016/j.apm.2011.09.073>
- 14 Yang, J. B., Jiang, L. J., and Chen, D. C. Dynamic modelling and control of a rotating Euler–Bernoulli beam, *J. Sound Vib.*, **274** (3–5), 863–875, (2004). [http://dx.doi.org/10.1016/s0022-460x\(03\)00611-4](http://dx.doi.org/10.1016/s0022-460x(03)00611-4)
- 15 Nayak, S., Bisoi, A., Dash, P. R., and Pradhan, P. K. Static stability of a viscoelastically supported asymmetric sandwich beam with thermal gradient, *Int. J. Adv. Struct. Eng.*, **6** (3), Article:65, (2014). <http://dx.doi.org/10.1007/s40091-014-0065-2>
- 16 Soltani, M., Asgarian, B., and Mohri, F. Elastic instability and free vibration analyses of tapered thin-walled beams by the power series method, *J. Constr. Steel Res.*, **96**, 106–126, (2014). <http://dx.doi.org/10.1016/j.jcsr.2013.11.001>
- 17 Bulut, G. Effect of taper ratio on parametric stability of a rotating tapered beam, *Eur. J. Mech. A Solids*, **37**, 344–350, (2013). <http://dx.doi.org/10.1016/j.euromechsol.2012.08.007>
- 18 Saito, H. and Otomi, K. Vibration and stability of elastically supported beams carrying an attached mass under axial and tangential loads, *J. Sound Vib.*, **62**, 257–266, (1976). [http://dx.doi.org/10.1016/0022-460x\(79\)90025-7](http://dx.doi.org/10.1016/0022-460x(79)90025-7)